BNL-225173-2024-TECH

EIC-ADD-TN-080

MBTRACK2 - APPLICATION ON EIC 5GEV ELECTRON RING REVERSE PHASE CONFIGURATION

X. Gu

January 2024

Electron-Ion Collider

Brookhaven National Laboratory

U.S. Department of Energy

USDOE Office of Science (SC), Nuclear Physics (NP)

DISCLAIMER

MBTRACK2-APPLICATION ON EIC 5GEV ELECTRON RING REVERSE PHASE CONFIGURATION

Xiaofeng Gu,* Alexei Blednykh, Michael Blaskiewicz

Collider Accelerator Department

Brookhaven National Lab

UPTON, NY 11973

xgu@bnl.gov

January 8, 2024

ABSTRACT

In this paper, we present a report on simulations conducted using the Mbtrack2 code for the 5GeV EIC Electron Storage Ring (ESR) RF system with a reversed phasing scheme. The Mbtrack2 code [1] has been thoroughly benchmarked, as described in references [2] and [3]. The simulation results presented in this paper include the beam loading effect but do not incorporate a feedback system.

***K*eywords**

RF dynamics, reverse phasing system, beam loading, mbtrack2

1 Introduction

The development of the Electron-Ion Collider (EIC) [4] at Brookhaven National Laboratory aims to study high-energy collisions by colliding polarized electron and polarized hadron beams, which will be stored in an Electron Storage Ring (ESR) and a Hadron Storage Ring (HSR), respectively.

According to the EIC design parameters, the electron beam energy will have three energy setups: 5 GeV, 10 GeV, and 18 GeV. One of the major challenges for the 5 GeV and 10 GeV ESR rings is the high power

*xgu@bnl.gov

Table 1: The parameters of 5 GeV ESR lattice calcualted from Bmad.

Parameters	value	unit	comments
E_0	5	GeV	Energy
L	3833.930	m	length
I_0	2.5	A	Average beam current
M	580		number of bunches
Q_x	40.120006		Tune
$Chrom_x$	1.195723		dQ/(dE/E)
J_x	1.004150		Damping Partition
ϵ_x	2.54404×10^{-8}	m rad	Emittance
α_x	9.55030×10^{-5}		Damping per turn
τ_x	1.33908×10^{-1}	Sec	Damping Time
Q_y	37.100001		Tune
$Chrom_y$	0.804365		dQ/(dE/E)
J_y	0.999908		Damping Partition
ϵ_y	2.89894×10^{-14}	m rad	Emittance
α_y	9.50996×10^{-5}		Damping per turn
τ_y	1.34476×10^{-1}	Sec	Damping Time
Q_z	6.25245E-02		Tune
σ_δ	5.18657E-04		equilibrium energy spread
U_0	9.51083E+05	eV/turn	Energy Loss
J_z	1.99503E+00		Damping Partition
α_z	1.89744E-04		Damping per turn
τ_z	6.73993E-02	second	Damping time
α_p	1.33646E-03		Momentum Compaction
η_p	1.33645E-03		Slip factor
γ_t	2.73540E+01		Gamma at transition
$I0$	1.15168E+05		synchrotron integral
$I1$	5.12889E+00		synchrotron integral
$I2$	1.08084E-01		synchrotron integral
$I3$	1.56153E-03		synchrotron integral

required to compensate for synchrotron radiation and beam-induced wakefields in the ESR. The synchrotron radiation power is approximately 10 MW at 2.5 A average current with 1160 bunches [4].

To address the beam loading effect caused by the significant synchrotron radiation power loss, a detuning frequency is required to compensate while accelerating the beam. Otherwise, the beam may experience Robinson instability [5] or other coupled-bunch instabilities.

To overcome this issue, a reversed phasing RF system is proposed, which employs two groups of cavities with the same RF cavity voltage but different synchronous phases. This approach reduces the required detuning frequency range and ensures stable beam operation.

It is worth noting that the reversed phasing RF system has already been successfully tested in the KEK B-Factory [6]. This suggests that the reversed phasing RF system is a viable option for the EIC project.

To validate and study the potential issues of the reversed phasing RF system for the EIC project, it has been examined using the Elegant code [5]. In this paper, a Python code named mbtrack2 [1] is used to study the reversed phasing RF system.

The paper is organized as follows. The first section of this paper describe the motivation of the RF reverse phase configuration via calcuating the detune frequency. The subsequent section presents simulatin setup which will be used in the later simulation. In the last section, we evaluate the bunch length, energy spread, and beam-induced voltage obtained from the Mbtrack2 code.

2 Motivation

The 5 GeV ESR lattice (version 5.3, Bmad format) is utilized for all the studies, and the lattice parameters are presented in Table 1.

In a electron storage ring, the natural energy spread σ_δ and bunch length σ_z are given by:

$$\begin{aligned} \sigma_\delta^2 &= Cq\gamma^2 \frac{I_3}{J_z I_2} \\ \sigma_z &= \frac{\alpha_p c}{\omega_s}\sigma_\delta \\ \omega_s &= \sqrt{\frac{eV_c h|\eta_p \sin\phi_s|}{2\pi\beta^2 E_0}} \end{aligned} \tag{1}$$

while $C_q = 3.832 \times 10^{-13} m$ and ω_s is the synchrotron tune of the storage ring with sin conversion. Or Eq. 1 can be modified as:

$$V_c|\eta_p \sin\phi_s| = \left(\frac{\alpha_p c}{\sigma_z}\sigma_\delta\right)^2 \frac{2\pi\beta^2 E_0}{eh} \tag{2}$$

After taking account another constrian of energy loss and the synchrotron phase, we can get

$$V_c cos\phi_s = U_0 \tag{3}$$

The energy loss per turn U_0 is listed in the table 1.

Then, by considering both Eq. 2 and Eq. 3, we can observe that the cavity voltage and phase are determined by the lattice and bunch length, which are the physical requirements of the EIC ESR ring. In Eq. 2 and Eq. 3, V_c represents the total cavity voltage.

Additionally, in certain operating scenarios characterized by high beam currents and low voltages, significant detuning of cavities is required to compensate for reactive beam loading. According to the second Robinson instability criterion discussed in [3], cavity detuning becomes necessary as it reduces the required RF power. The detuning frequency can be obtained from the following equations.

$$\begin{aligned} tan\psi &= -\frac{V_{br}}{V_c} sin\phi_s \\ V_{br} &= 2I_0 R_L \\ tan\psi &= 2Q_L \frac{\Delta\omega}{\omega_c} = 2Q_L \frac{\Delta f}{f_{RF}} \end{aligned} \tag{4}$$

Therefore, we can calculate the detuning frequency as follows:

$$\Delta f = \frac{f_{RF} I_0 \sin(\phi_s)(\text{RoQ})}{V_c} \tag{5}$$

Here, V_c represents the voltage of a single cavity in Eq. 5 and Eq. 6, while ϕ_s and V_c are calcuated from Eq. 2 and Eq. 3.

Detuning is necessary to reduce the required RF power. However, excessive detuning can result in coupled bunch instabilities. Narrow resonances located at the synchrotron sidebands may excite longitudinal coupled-bunch instabilities. While these resonances primarily originate from the higher-order modes of the cavities, some may also arise from the revolution harmonics of the beam loading voltage due to asymmetric fill in the stored beam. These harmonic lines possess finite widths due to the energy spread of the bunches and the synchrotron oscillations that develop as a result of RF phase offsets. Consequently, these harmonic components of the beam loading voltage can drive coupled-bunch instabilities, and their elimination through comb-filter shape feedback is crucial.

Detuning often causes the peak of the intrinsic resonant frequency of the cavities to shift by more than one revolution harmonic. Table 2 provides the detuning frequency calculated with the normal RF phase configuration and a reverse phase configuration [7].

We observe that the detuning frequency is -216.0 kHz. However, the revolution frequency of the collider ring is only 78 kHz. In other words, the resonant impedance of the cavities would occur between $f_{rf} - 3f_0$ and $f_{rf} - 2f_0$. Such impedance could drive longitudinal coupled-bunch instabilities with significant strength. Conversely, with the reverse phase configuration, the detuning frequency is approximately -15 kHz, which is much less than the revolution frequency of 78 kHz. Consequently, the longitudinal coupled-bunch instabilities can be avoided with this configuration.

To evaluate and validate the reverse phase RF configuration, particle tracking was performed using the mbtrack2 code, which includes the beam loading effect, as described in this paper.

Table 2: The Detuning Frequency for the 5 GeV ERS 591MHz Cavities

Parameters	Normal Configuration	Reverse Phase Configuration	unit
I_{beam}	2.5	2.5	A
P_{beam}	4.42	4.42	MV
bucket Height	5.5	5.5	1E-3
$Cavities[F]$	17	9	
V_{sync}	1.55	0.82	MV
$V_{total}[V_{cav}]$	4.6 [0.27]	37.5[4.17]	MV
ϕ_s	160.3	178.7	deg
$Detuning$	-216.0	-14.9	kHz
$Cavities[D]$	-	8	
V_{sync}	-	0.73	MV
$V_{total}[V_{cav}]$	-	33.2[4.15]	MV
ϕ_s	-	1.3	deg
$Detuning$	-	15.0	kHz

3 Simulation Setup in Mbtrack2

To ensure accurate simulation results and minimize simulation time, this section evaluates the parameter setup in Mbtrack2. These parameters encompass the number of bins and the number of macro-particles within a single bunch, along with the total number of bunches within the ring.

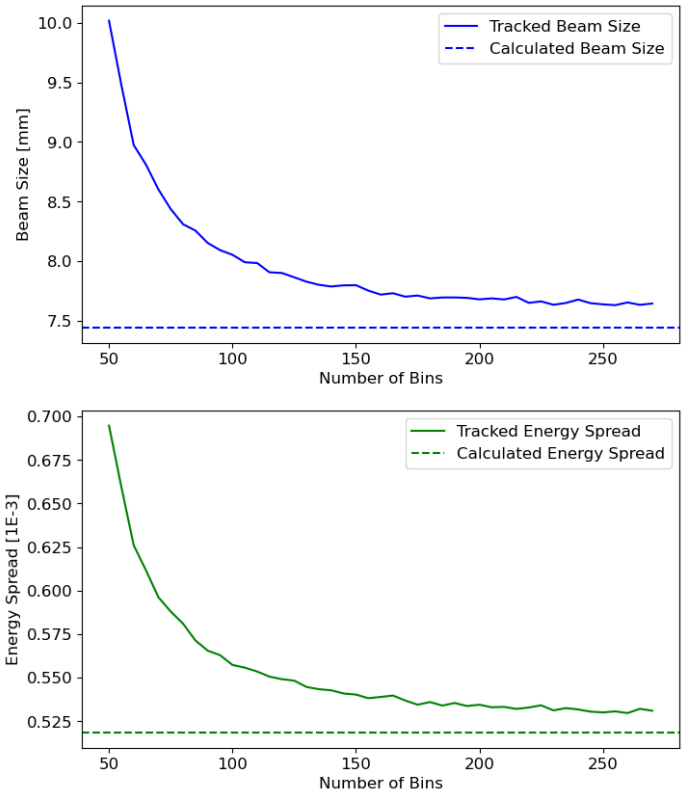

Fig. 1: The plot demonstrates the variation of beam length and energy spread as a function of the number of bins in a bunch. It is evident that increasing the number of bins leads to values that are closer to their intended values. The analysis presented in the paper employed a value of 200 bins for this purpose.

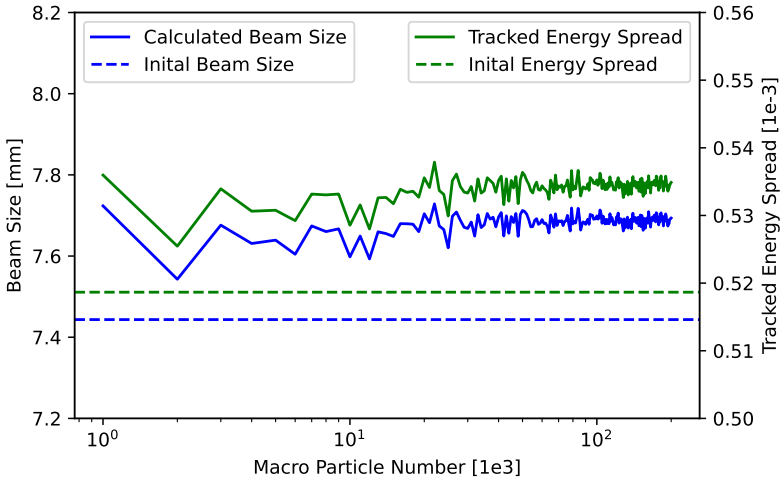

Fig. 2: he plot demonstrates the variations in beam length and energy spread as a function of the number of macro-particles. Based on the plot, a macro-particle number of 1E4 is deemed sufficient to obtain accurate results. These simulations were conducted using three focusing RF cavities.

For this evaluation, a reverse phase configuration employing 10 focusing RF cavities and 5 defocusing RF cavities is utilized. The corresponding parameters for this configuration are presented in Table 3.

3.1 Number of Bins

To perform RF dynamics tracking using the CavityResonator method in the Mbtrack2 code, it is crucial to accurately set up the bin number and the total number of macro-particles in a bunch.

Fig. 1 demonstrates how the beam length and energy spread vary with the number of bunch bins. As the number of bins in a bunch increases, the beam length and energy spread approach their designed values more closely. In this paper, we utilized a bin number of 200. For the simulation described above, three focusing CavityResonator cavities, each with a voltage of 3.35E6 Volt, were employed.

3.2 Number of Macro-particles

The number of macro-particles in a bunch is another important parameter for obtaining accurate simulation results.

Fig. 2 illustrates how the beam length and energy spread vary with the number of macro-particles in a bunch. It can be observed that a macro-particle number of 1E4 is sufficient to achieve accurate results. This is further supported by another simulation investigating the variation of beam length along the bunch train, as shown in Fig. 3. Therefore, a macro-particle number of 1E4 is initially employed to expedite the simulation process, and subsequently, these results are reviewed to conduct more detailed studies using a macro-particle number of 5E4.

Table 3: RF parameters for mbtrack2 Simulation setup

Parameter	10 Focusing Cavity	5 Defocusing Cavity
m	1	1
N_{cav}	10	5
Q	2e+10	2e+10
RoQ	37	37
$R_{s\_per\_cavity}$ [Ω]	7.4e+11	7.4e+11
R_s [Ω]	7.4e+12	3.7e+12
β	2.19784e+04	2.19784e+04
Q_L	9.09944e+05	9.09944e+05
R_L	33667928	33667928
$detune$ [Hz]	-1.63399e+04	1.63404e+04
f_c [Hz]	5.91134e+08	5.91167e+08
ω_c [rad/s]	3.71421e+09	3.71441e+09
ψ [deg]	-88.86	88.86
V_c [V]	3.35e+07	1.675e+07
θ_s [deg]	88.86	-88.86
V_g [V]	1.33158e+06	6.65788e+05
θ_g rad	1.80814e-06	-1.80829e-06
V_{gr} [V]	6.6997e+07	3.34985e+07
θ_{gr} [deg]	88.86	-88.86
V_b [V]	3.35e+07	1.675e+07
V_{br} [V]	1.68552e+09	8.42759e+08
P_g [W]	1.66657e+06	8.33285e+05
P_c [W]	7.58277e+01	3.79139e+01
P_b [W]	1.66649e+06	8.33247e+05
P_r [W]	2.51703e-10	9.43601e-12
n_{bin}	200	200
Filling time [s]	4.89980e-04	4.89953e-04
Loss factor [V/C]	6.87128e+11	3.43583e+11

The plot demonstrates the beam length and energy spread for macro-particle numbers of 1E4, 3E4, and 1E5 in a bunch. The total number of bunches equally distributed around the ring is 290. These results are obtained from simulations involving 10 focusing cavities and 5 defocusing cavities. Additionally, the plot depicts the beam length and energy spread along the bunch train for different total bunch numbers. These bunches are equally distributed around the ring.

From Fig. 3, it is also evident that simulations with fewer macro-particles exhibit higher noise or deviation in the bunch length and energy results. However, as the number of macro-particles increases, these deviations become smaller. To reduce these deviations or noise, it is recommended to employ different seeded simulations.

Furthermore, a strong correlation can be observed between bunch length and energy simulations.

3.3 Number of Bunches

In addition to the number of bins and the number of macro-particles in a bunch, reducing the simulation time necessitates a smaller number of bunches. Hence, a comparison is made between three bunch trains with a total bunch number of 290, 580, and 1160.

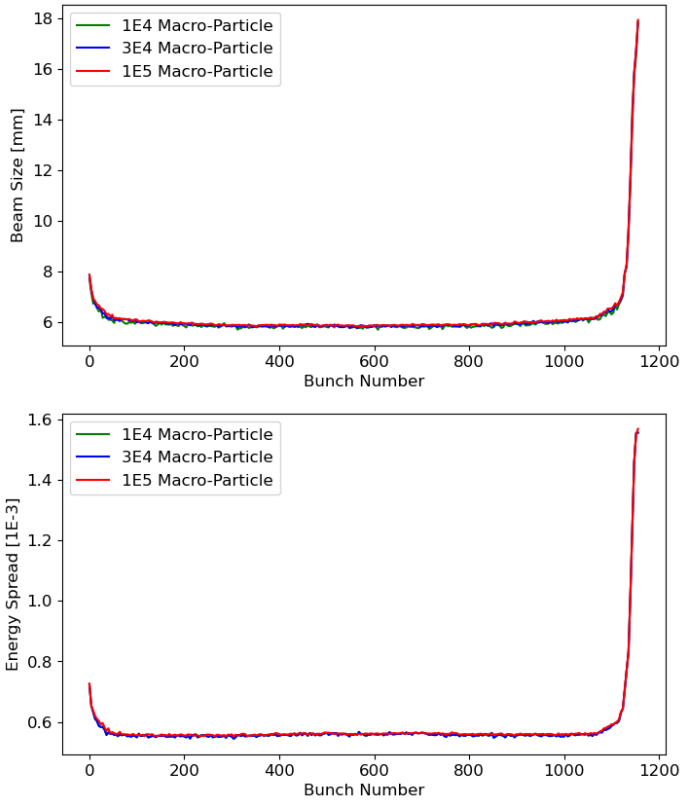

Fig. 3: The beam length and energy spread vary with the number of macro-particle in a bunch.

Fig. 4 illustrates that these three setups for bunch numbers are nearly identical in the middle of the bunch train. Although some discrepancies can be observed at the two ends, they are not significant. Therefore, to expedite the simulation process, a bunch number of 290 is chosen, while a total bunch number of 580 or 1160 will be used for the final results.

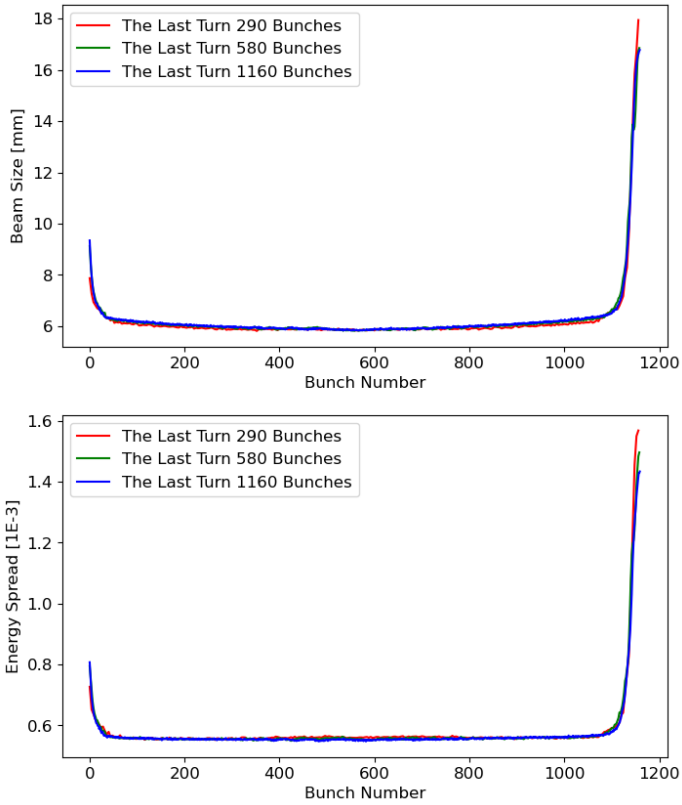

Fig. 4: Variation of beam length and energy spread in a bunch train with the number of macro-particles.

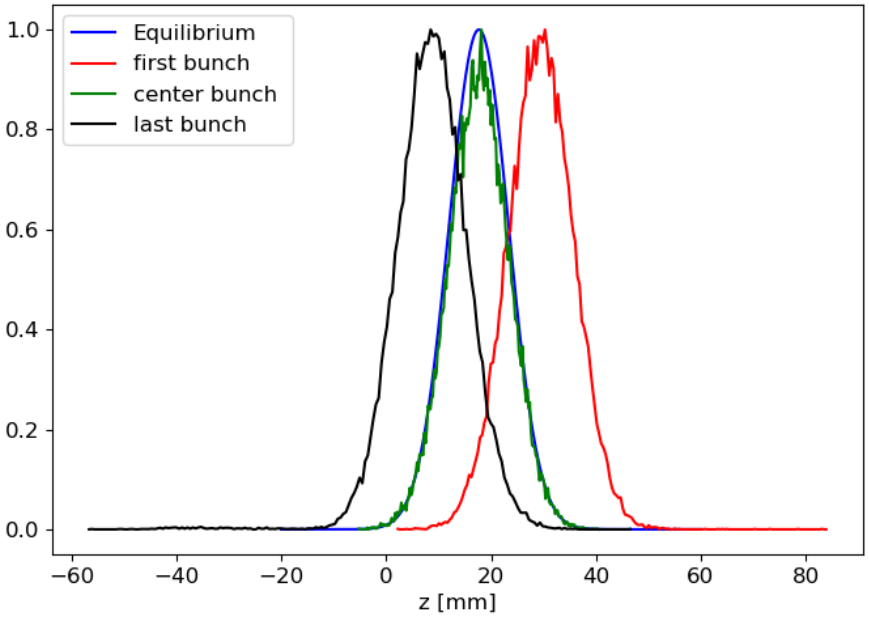

Fig. 5: The variation of beam length and energy spread in a bunch train with the number of macro-particles is investigated.

4 Mbtrack2 Simulation for 5GeV EIC reverse phase configration

4.1 10F-5D reverse phase configuration

4.2 Bunch length, bunch positoin and energy spread

By employing the same parameter setup as presented in Table 3 for the ten focusing cavities and five defocusing cavities, we can obtain the bunch length distribution, bunch longitudinal position, and energy spread along the bunch train.

Firstly, we compare the bunch profile, bunch length, and longitudinal position between tracking and equilibrium state calculations using two RF systems [8] and [9]. Fig. 5 displays the equilibrium profile and the tracked profile of the center bunch (in the 290-bunch train) using 5.0×10^4 macro-particles. It is evident that the bunch's longitudinal position and profile exhibit excellent agreement. A higher number of macro-particles is necessary to obtain a smoother tracked profile.

Fig. 6 presents the results of simulations with 290 bunches, 5E4 macro-particles, and 20 k turns. The single cavity voltage is 3.35 MV, and the synchrotron phase is 88.86 degrees (178.86 degrees for cosine conversion).

The theoretical design values for bunch length and energy spread are indicated by the red solid lines in the figure. The bunch length is also evaluated using the equilibrium profile (represented by the red dashed line). The theoretical longitudinal bunch position for the two RF systems is calculated based on the equilibrium state formula in [8] and [9]. The energy spread is determined by the lattice itself.

From the top plot of Fig. 6, it is evident that the bunch length exhibits an asymmetric parabolic shape for different bunch indices in a bunch train. The bunch length at the end of the bunch train is slightly larger than at the beginning. This result is consistent with the findings in [5]. The middle plot reveals that the centroid of the bunch train has a shift of 17.68 mm, displaying a linear distribution for the different bunches in the train. Additionally, the bunch energy spread is 5.5×10^{-4}, which is very close to the design value of 5.2×10^{-4}.

From these plots, we observe that the simulated bunch length, longitudinal bunch centroid, and bunch energy spread closely match their theoretical values. Hence, we demonstrate that the mbtrack2 code accurately simulates these parameters, including the beam loading effect.

4.3 Stable Region

Fig. 7 shows the results with different single cavity voltage setups of 2.7MV, 3.0MV, and 3.4MV with a phase of 87.5 degrees (177.5 degrees for cos conversion). From the plot, we can see that if the cavity voltage is too low, the beam starts to become unstable. It appears that the synchrotron phase angle dominates the longitudinal centroid position. The stable region with different cavity voltage and synchrotron phase will be discussed later.

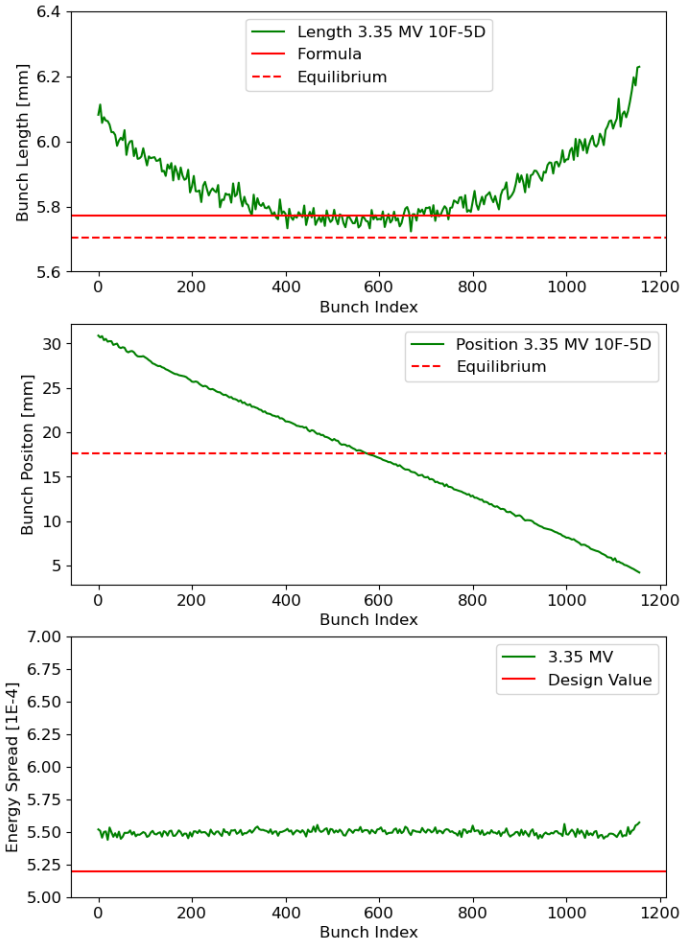

Fig. 6: The beam length (top), bunch position (middle), and energy spread (bottom) depend on the index of the bunch within a bunch train.

Fig. 8 illustrates the dependence of bunch length, bunch position, detune frequency, and energy spread on the synchrotron phase, considering different single cavity voltages for a configuration with 10 focusing and 5 defocusing reverse phases. The dashed lines represent the tracked results, while the solid lines correspond to the calculated results. The bunch length is calculated using Eq. 1, and the bunch position is determined using the equilibrium method (refer to [8] and [9]).

Firstly, analyzing the plots for the bunch length, bunch position, and energy spread simulation results, we observe the presence of a stable region for the cavity voltage. When the single cavity voltage is below 2.4 MV, the simulation results become unstable. On the other hand, if the single cavity voltage is 3.8 MV, the parameters exceed the range depicted in these plots, resulting in an unstable beam. The stable region can be identified between 2.6 MV and 3.6 MV.

Secondly, the simulation reveals a stable region for the cavity phase as well. If the phase becomes closer to 90 degrees for each cavity voltage setup, instability arises. For instance, for the single cavity voltage setup of 3.6

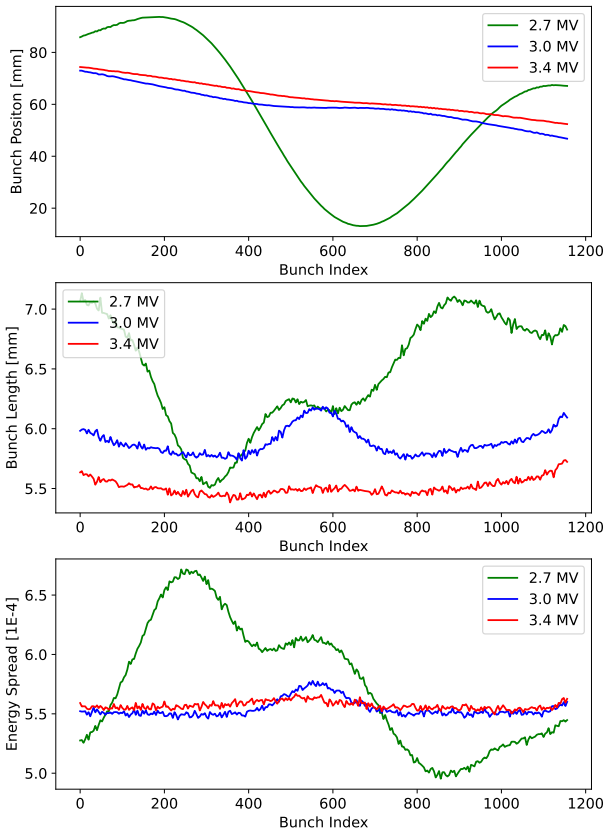

Fig. 7: The plots illustrate the variation of beam length (top), bunch position (middle), and energy spread (bottom) with respect to the bunch index in a bunch train.

MV, the upper limit for the phase is 89 degrees (excluding this point), which is why no data point is shown in this figure due to the beam's instability.

Thirdly, we observe that the bunch position increases as the synchrotron phase deviates to the left from 90 degrees. However, the unstable region also exhibits a lower limit, providing a clue for the single cavity voltage of 2.4 MV. Additional simulation points are required for other voltages.

4.4 Cavity Voltage and Phase

The total voltage and phase for 10 focusing cavities and 5 defocusing cavities are shown in Fig. 9, Fig. 10, Fig. 11, and Fig. 12, respectively.

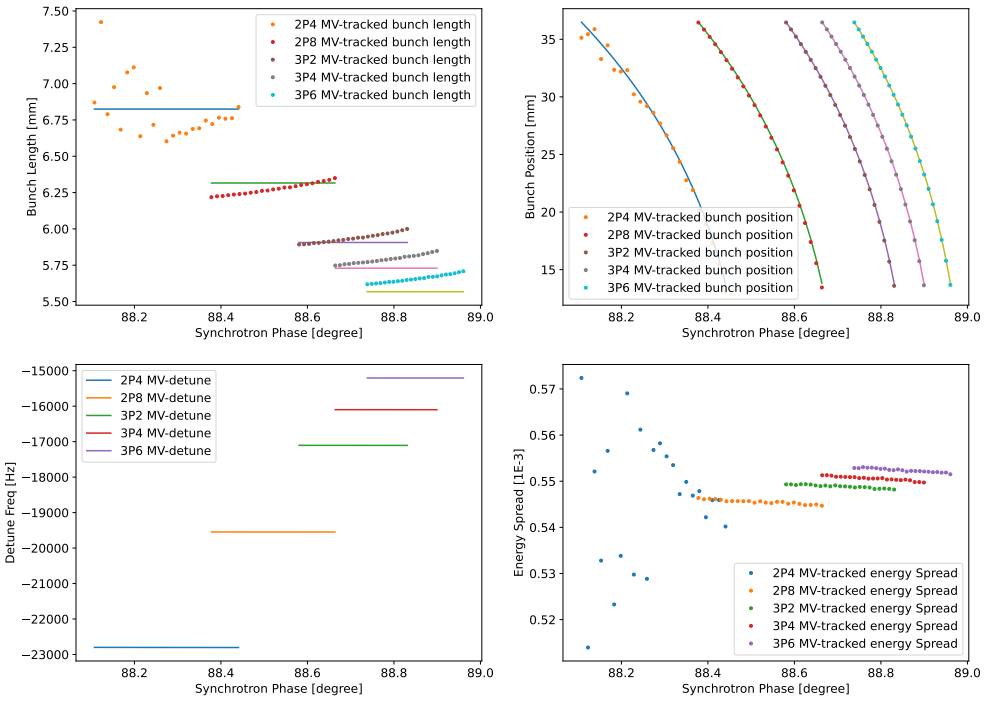

Fig. 8: The plot displays the bunch length, bunch position, detune frequency, and energy spread as functions of cavity phase and voltage for the 10F-5D reverse phase configuration.

For the cavity voltage of the 10 focusing cavities, Fig. 9 illustrates that the voltage follows a parabolic shape, reaching its maximum value at the center of the bunch train. Conversely, the cavity voltage of the 5 defocusing cavities exhibits a minimum value at the center of the bunch train due to the reverse phase.

Regarding the phase change, it is non-linear with respect to the bunch index number. Based on the simulation results mentioned above, the phase change for both cavity configurations is approximately 6 degrees.

In the case of a continuous beam with constant intensity and a gap of length $\Delta T = \frac{100}{1260} T_0$, we can derive a linear phase variation with a maximum excursion using the following formula [10]:

$$\Delta\phi_{\text{max}} = 2\pi\Delta f \cdot \Delta T \tag{6}$$

Here, Δf is obtained from Eq. 5 or table 3. By utilizing this formula, we can estimate the maximum phase change to be 5.97 degrees, which closely aligns with the values presented in Fig. 9 and Fig. 11.

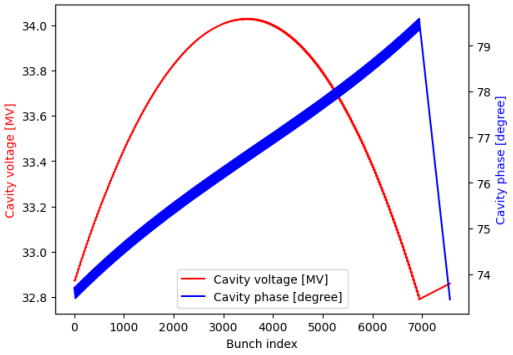

Fig. 9: The 10 focusing cavity total voltage and phase vary with the bunch index.

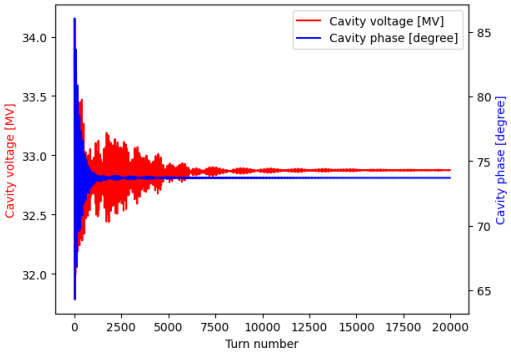

Fig. 10: The 10 focusing cavity total voltage vary with simulation turns.

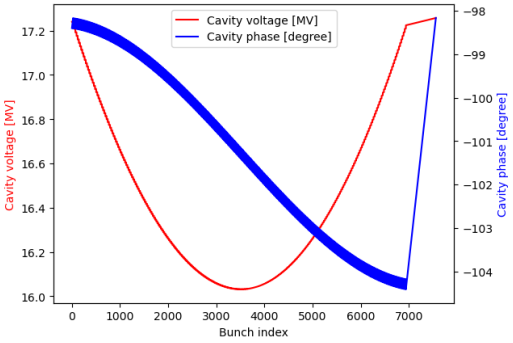

Fig. 11: The 5 defoucsing cavity total voltage and phase vary with the bunch index.

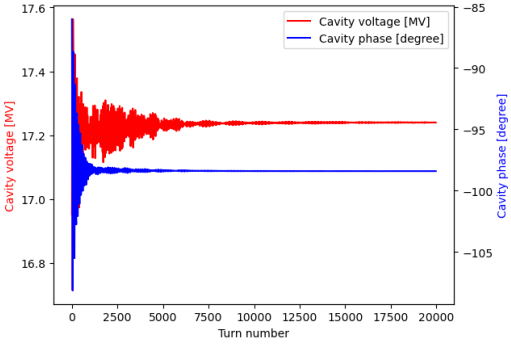

Fig. 12: The 5 defoucsing cavity total voltage vary with simulation turns.

5 Summary and Discussion

In this paper, the 5 GeV ESR ring reverse phase configuration is simulated using mbtrack2.

Using the 10F-5D configuration, we found from Fig. 6 that the beam size has a parabolic shape along the bunch train. The bunch at the center of the bunch train has the minimum bunch length. Therefore, the bunch length simulations in this paper are very close to the previous results (EIC CDR [4] and Alexei [5]), which used the 12F-6D and 10F-7D configurations.

The same figure also shows that the centroid of the bunch has a very close linear relationship with the bunch index number. The simulation results about the centroid of the bunch are also very close to the previous results (EIC CDR [4] and Alexei [5]), although they have different RF parameter setups.

In addition, the whole bunch train is shifted to a position of 17.68 mm. This was not mentioned in the previous two documents.

For the 10F-5D configuration, there is a stable region for both the cavity voltage and synchrotron phase. We also found that other configurations, such as 10F-6D and 10F-7D, have a narrower stable region than 10F-5D.

In other words, using the same parameters (10F-7D) as Alexei [5] used, we cannot obtain the same plots because the bunches are not stable.

Therefore, the results from the three methods do not agree quantitatively, but they do agree qualitatively. To find the reasons for the different results, we need to make more efforts to understand all three methods.

From the three simulation methods, although they have different RF parameters settings, we didn't find a shows topper for the reverse phase configuration presently. However, there is a bunch train centroid shift (17.68 mm) from the simulation in this paper.

All the results in this paper were obtained without any feedback system, which needs to be studied in the next step.

References

[1] https://gitlab.synchrotron-soleil.fr/PA/collective-effects/mbtrack2

[2] doi:10.18429/JACoW-IPAC2021-MOPAB070, IPAC2021, Campinas, SP, Brazi

[3] EIC Tech Note: EIC-ADD-TN-066

[4] Electron Ion Collider Conceptual Design Report 2021, https://www.osti.gov/biblio/1765663

[5] Simulation of the RF system with reversed phasing, BNL-223347-2022-TECH

[6] Y. Morita et al, Proc. 14th Int. workshop on SRF, Berlin Germany, 236 2009

[7] Kevin S. Smith APEX Workshop, November 9, 2021 https://indico.bnl.gov/event/13401/

[8] Gamelin, Alexis, and Naoto Yamamoto. "Equilibrium Bunch Density Distribution with Multiple Active and Passive RF Cavities." 12th International Particle Accelerator Conference. 2021.

[9] Venturini, M. (2018). Passive higher-harmonic rf cavities with general settings and multibunch instabilities in electron storage rings. Physical Review Accelerators and Beams, 21(11), 114404.

[10] D. Boussar, PAC1991, p2447

6 Appendix

Fig. 13 depicts the variation of bunch length and energy spread with simulation turns for a single cavity voltage of 3.35 MV. It can be observed that there is a significant increase in bunch length and energy spread at the beginning of the simulation for both the first and last bunches. However, after approximately 20,000 turns, both values converge close to the theoretical value.

This distortion in bunch length and energy spread for the first and last bunches is believed to be an artificial effect of the simulation. The beam-induced voltage affects all bunches from the beginning of the simulation, without assuming any bunching injection or current ramp-up. This artificial effect can be reduced through fine-tuning of simulation methods.

In Fig. 14, the evaluation of bunch length and energy spread for the center bunch is shown as a function of simulation turns, with a single cavity voltage of 3.35 MV.

Fig. 15 illustrates the variation of bunch length, bunch position, and energy spread as a function of bunch index for three different cavity voltages. Meanwhile, Fig. 16 showcases the variation of first, center, and last bunch length, as well as energy spread, with simulation turns for a single cavity voltage of 3.20 MV.

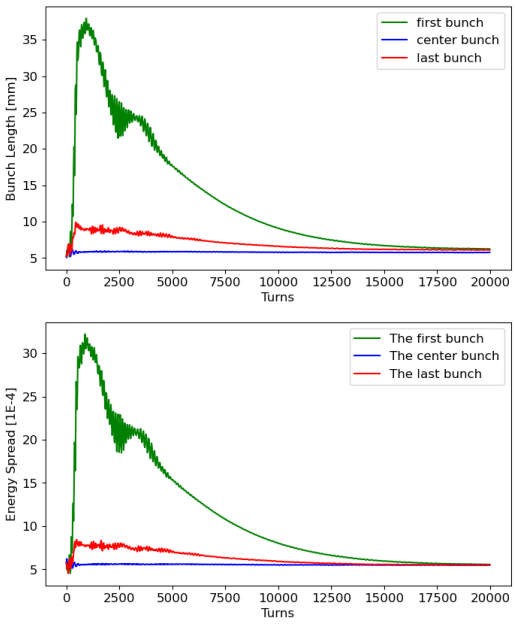

Fig. 13: The bunch length and energy spread vary with simulation turns for 3.35 MV single cavity voltage.

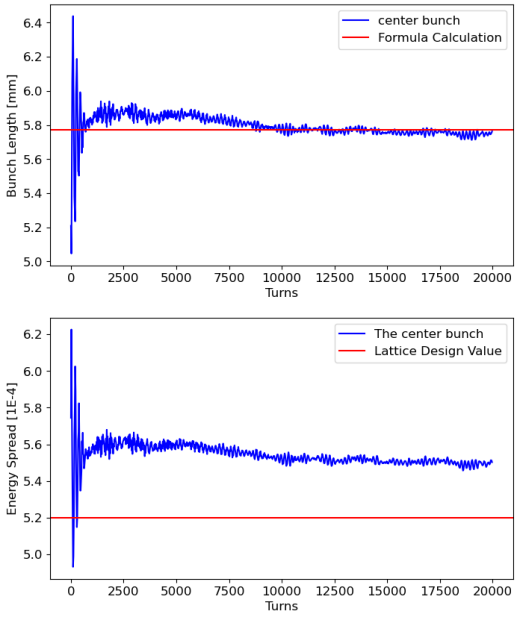

Fig. 14: The center bunch length and energy spread vary with simulation turns for 3.35 MV single cavity voltage.

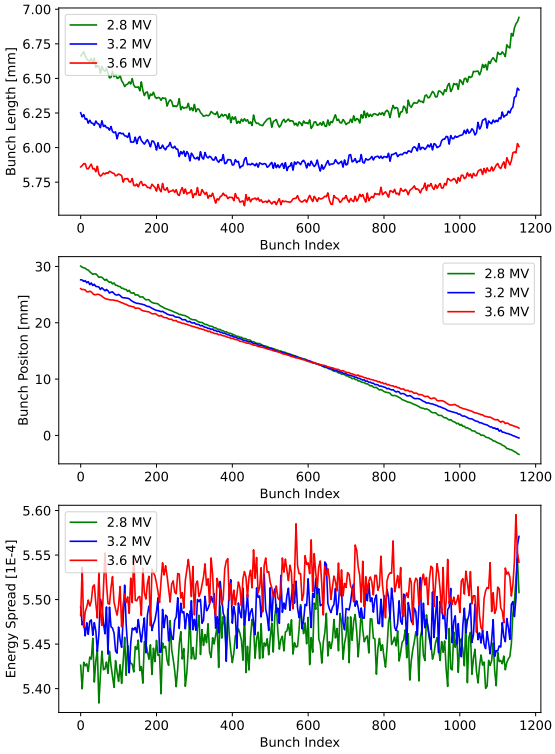

Fig. 15: The bunch length, position and energy spread vary with bunch indext for the 10F-5D configuration with 3.35 MV single cavity voltage.

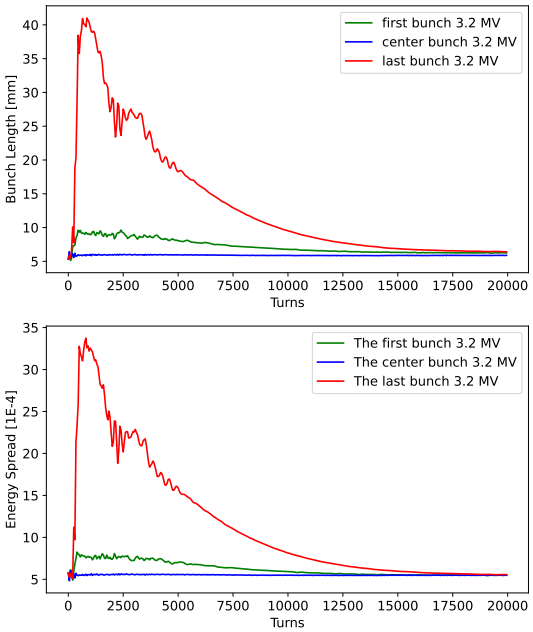

Fig. 16: The bunch length and energy spread vary with simulation turns for the 10F-5D configuration with 3.35 MV single cavity voltage.